3.1 General information about project B2

3.1.1 Title: Dynamics of quantum dot based multi-section laser and amplifier structures

3.1.2 Research areas: Theoretical Physics/ Nonlinear dynamics and control, laser simulations

3.1.3 Principal investigators

Schöll, Eckehard, Prof. Dr. rer. nat., PhD, 06.02.1951, German
Technische Universität Berlin
Institut für Theoretische Physik , Sekretariat EW 7-1
Hardenbergstraße 36
10623 Berlin
Phone: +49 30 314 23500
E-Mail: schoell@physik.tu-berlin.de

Does the above mentioned person hold a permanent position?
Yes

Lüdge, Kathy, Dr. rer. nat., 17.01.1976, German
Technische Universität Berlin
Institut für Theoretische Physik, Sekretariat EW 7-1
Hardenbergstraße 36
10623 Berlin
Phone: +49 30 314 23002
E-Mail: luedge@physik.tu-berlin.de

Does the above mentioned person hold a permanent position?
No Position limited until 11/2011
Further employment is planned until 12/2015.

3.2 Summary

In this project we will investigate the nonlinear dynamics of electrically pumped quantum dot based semiconductor laser and amplifier structures. The focus will be on physical modeling and numerical simulations of multi-section devices with integrated electro-optic modulator-, absorber- and feedback sections, as well as on optically injected devices. Based on our work funded during the last period, regarding simple Fabry-Perot lasers, we will extend our studies to more complex integrated structures where multiple time delay effects play an important role.

We will develop microscopically based models that are able to quantitatively describe the complex integrated structures and at the same time still allow for analytic insights. The nonlinear dynamics and bifurcation scenarios of laser structures will be described by rate equations incorporating ground and excited quantum dot states of electrons and holes as well as the electron and hole densities in the carrier reservoir. For the amplifier structures a semiconductor Bloch equation approach that describes the coupled polarization and population dynamics will allow us to extract and predict important device parameters like chirp, amplitude-phase coupling and cavity detuning. Furthermore, noise effects will be investigated.

3.3 Project development

3.3.1 Report and state of the art

Two subtasks were investigated in the preceding period of the project:

(i) Electrically modulated edge-emitting quantum dot lasers

A microscopic 5-variable model for quantum dot (QD) lasers, based upon the coupled dynamics of photons, and electrons and holes in the QDs and in the surrounding quantum well (QW) acting as a carrier reservoir was developed [P5, P7, P8]. One goal was the quantitative modeling of the turn-on dynamics and the modulation response of directly modulated edge-emitting QD lasers (a schematic sketch of the laser and the band structure is shown in Fig.2(a) and (b)). To achieve this goal we have extended our microscopic rate equation

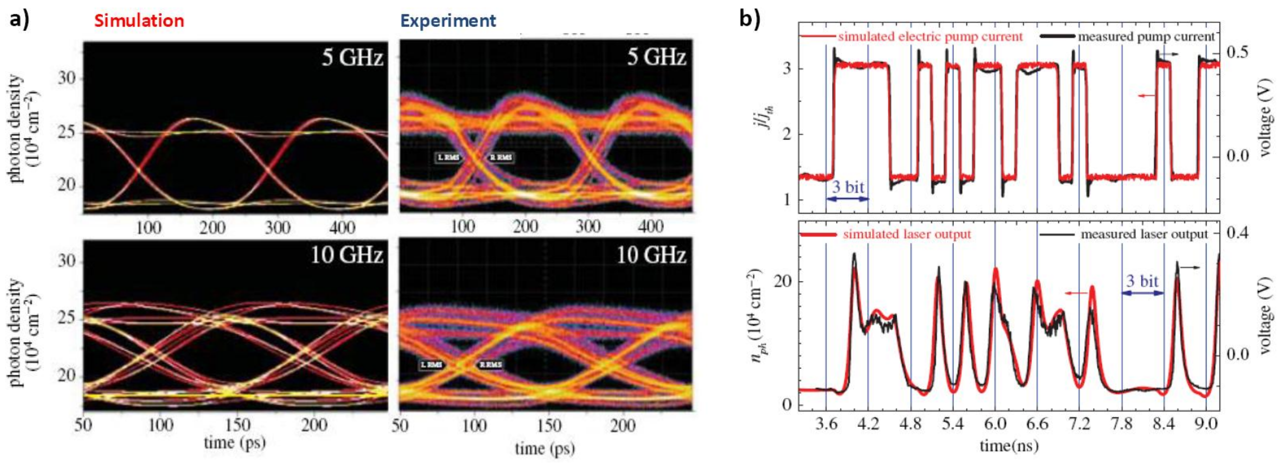

Fig. 1: (a) Simulated and measured eye pattern diagrams for pump currents switching between 4 j_{th} and 6 j_{th} (j_{th}: threshold current density) for bit repetition frequencies of 5 GHz and 10 GHz (b) Simulated (red line) and measured (black line) laser output (bottom) driven by an electric pump signal (top). After [P2].

model by including heating effects, pump-dependent spectral properties, and Auger recombination losses in the carrier reservoir [P2]. This has not been done by merely including a static dependence upon the pump current, but rather by a fully self-consistent dynamic dependence on the temperature, the number of longitudinal modes, and the loss rate upon the carrier densities in the reservoir. The latter is calculated dynamically from the coupled rate equations in dependence upon the pump current. Thus we could not only describe correctly the current dependence under continuous-wave (cw) operation, but also predict the transient large-signal response over a large range of pump currents. Figure 1b depicts the simulated and measured laser response to a bit sequence showing the very good quantitative agreement. The quantitative power of the modelling can also be seen by comparing the results to experimental eye diagrams at the emission wavelength of 1.3 µm obtained within the project C6 (Bimberg, Erbert) (see Fig. 1a). We have found that decreasing the injection efficiency into the QW and increasing carrier losses inside the QW at high QW carrier densities is crucial in order to correctly model the large-signal response of the QD laser. Furthermore we have found that an increasing temperature leads to a reduction of the relaxation oscillation frequency and thus to a reduction of the modulation bandwidth at higher pump currents [P2].

Regarding the microscopic basis of our rate equation model we have found that the details of the energy scheme of the QD-QW system sensitively influence the microscopically calculated nonlinear Coulomb scattering rates, and hence the nonlinear turn-on dynamics. We have systematically studied the effects of the electron and hole confinement energies and zero-point energies as well as the doping of the carrier reservoir [P5], and thus we are able to predict changes in the laser dynamics induced by changes in the QD size or QD composition.

A crucial issue for rate equation models is the relation between in- and out-scattering rates. For single-carrier processes in simple two level systems the ratio is constant and only depends upon the temperature T. However, we have derived the detailed balance formula $S_{e/h}^{in,cap} = S_{e/h}^{out,cap} \exp\left[\frac{\Delta E_{e/h}}{kT}\right]\left[\exp\left[\frac{w_{e/h}}{\rho_{e/h}kT}\right]-1\right]$ connecting the non-equilibrium in- and out-scattering Auger rates $S_{e/h}$ (direct capture processes) via a factor that depends on the carrier density $w_{e/h}$ in the carrier reservoir [P7] ($\Delta E_{e/h}$ is the energetic distance between the band

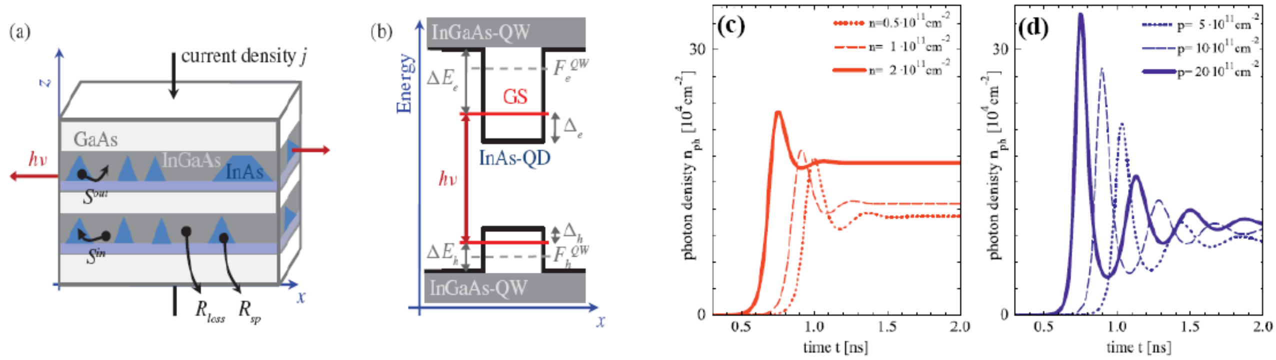

Fig. 2: (a) Sketch of the QD laser structure and (b) of the resulting energy band diagram. (c) and (d) show time series of the photon density during laser turn-on for different n-doping density (c) and different p-doping density (d). Dotted, dashed and solid lines correspond to doping of 0.1, 0.2 and 0.4 times the degeneracy concentration, respectively. Pump current $j = 2.5\, j_{th}$. After [P2, P5].

edge of the reservoir and the confined QD level. The degeneracy concentration of electrons (e) and holes (h) in the reservoir is denoted by $\rho_{e/h}\, kT$ with the 2D density of states $\rho_{e/h}$. We have shown that the inclusion of separate dynamics of holes and electrons is essential in order to explain the dynamic behaviour of a QD laser with a doped carrier reservoir. The dynamics of electrons and holes becomes the more synchronized, the more similar the scattering times (given by the inverse scattering rates) are. However, introducing p-doping drastically reduces the damping of the turn-on relaxation oscillations (see Fig.2d), which is a significant feature influencing the modulation response of these QD lasers [P5]. On the other hand, n-doping increases the damping (Fig.2c).

We have also investigated many-body and non-equilibrium effects upon the dynamical behavior of a QD laser diode. Simulations, based on the Maxwell-Semiconductor-Bloch equations, show strong dependence of the turn-on delay on initial cavity detuning Δ_0 (see Fig.3). This is due to a dynamical shift in the quantum dot distribution caused by bandgap renormalization [P1]. Gain switching behavior is found to be insensitive to inhomogeneous broadening, because the balancing between many-body and free-carrier effects inhibits a cavity resonance walk-off. Both the relaxation oscillation damping and frequency are found to increase with decreasing inhomogeneous broadening widths. However, in contrast to bulk and quantum-well lasers, oscillation damping increases less than the frequency. For applications where control or reproducibility of the turn-on delay is important, it is crucial to have the proper initial cavity detuning with respect to the QD distribution.

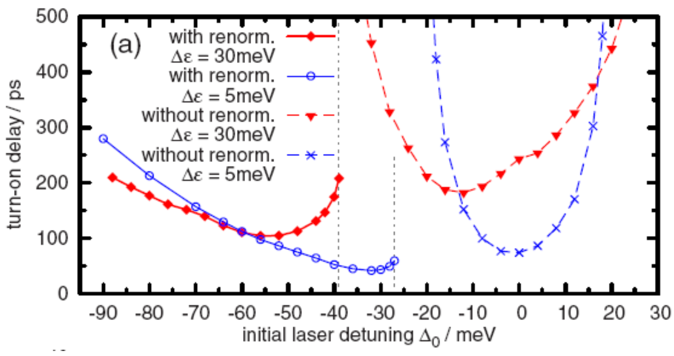

Fig. 3: Turn-on delay vs. initial cavity detuning with (solid) and without (dashed) many-body effects for inhomogeneous broadening of 5 and 30 meV. After [P1].

Another goal of our project was the investigation of a quantum dot laser subjected to optical feedback. For this purpose we combined a Lang-Kobayashi like field equation with the microscopically based carrier rate equations. By tuning the phase-amplitude coupling and the optical confinement factor we were able to discuss various scenarios of the dynamics, and compare them with conventional quantum well lasers. Due to the optical feedback, multistability occurs in our model in form of external cavity modes or delay-induced intensity pulsations. External cavity modes are the basic solutions of the dynamical equations having constant carrier and photon densities and a phase that varies linearly in time. Thus they correspond to cw operation of the laser with feedback. In dependence of the feedback strength we analyzed complex bifurcation scenarios for the intensity of the emitted laser light as well as time series, power spectra and phase portraits of all dynamic variables in order to elucidate the internal dynamics of the laser [P6]. Further we compared our QD to a QW model consisting of a similar field equation but only one carrier-equation for the density of electron-hole pairs. We found that for the same damping of the relaxation oscillations (RO) both lasers become unstable at the same value of the feedback strength in a supercritical Hopf bifurcation. As a result we could explain the reduced feedback sensitivity found in QD devices on the one hand by their strongly damped relaxation oscillations and on the other hand by the relatively small number of external cavity modes for a given external cavity round trip time. The small number of external cavity modes originates from a weaker phase-amplitude coupling modelled by smaller linewidth enhancement factor (α-factor [1,2]) com-

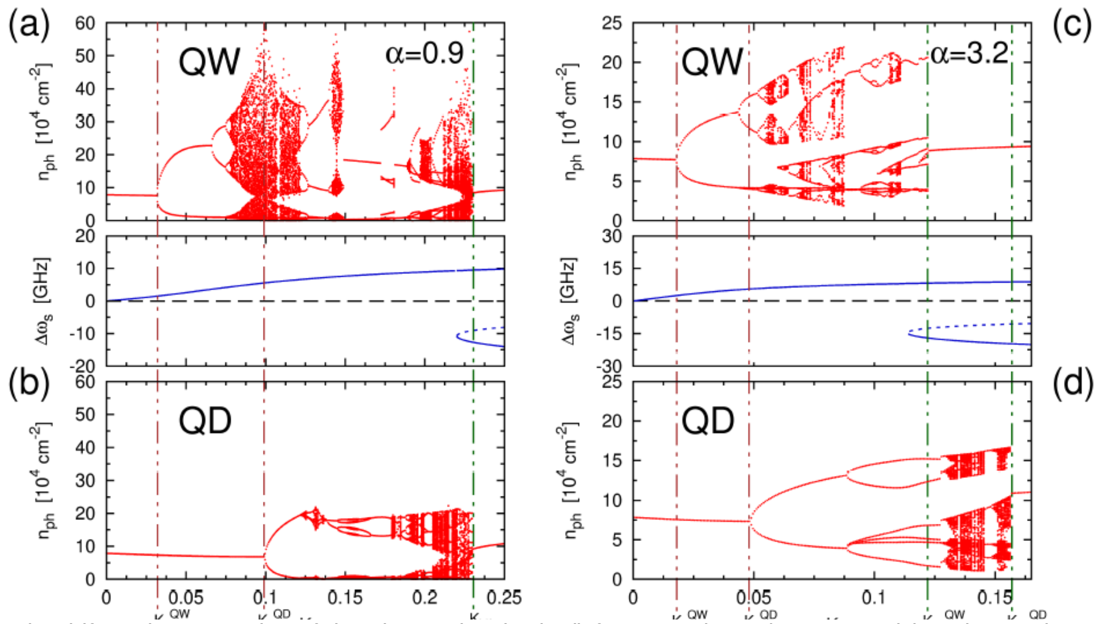

Fig. 4: First bifurcation cascades of the photon density (red) for a QW laser (upper panels) and a QD laser (lower panels) in dependence of the feedback strength K for α=0.9 ((a)-(b)) and α= 3.2 ((c)-(d)). Middle panels: Frequency deviations of the possible external cavity modes (blue). Brown vertical dash-dotted lines mark the Hopf bifurcation. Green vertical dash-dotted lines mark the ends of the bifurcation cascades. After [P6].

pared to quantum well devices [P6]. For QD lasers with large α-factor we found bifurcation cascades leading to chaotic regions alternating with short regions of stable cw operation. This resembles the behavior typical for QW devices. For low α-factor the model exhibits reduced feedback sensitivity and performs stable cw operation over a wide range of increasing feedback strength (Fig. 4). Moreover, for low α-factor we found intensity pulsations in a certain range of the feedback strength, which can be strictly regular. They become more irregular with increasing α-factor.

Since the systematic numerical study of the QD laser with optical feedback revealed that damping Γ_{RO} and frequency ω_{RO} of the relaxation oscillations (RO) are crucial for the feedback sensitivity we performed analytical investigations that aimed at understanding the interplay between scattering times and relaxation oscillations. Our analytical approximations are in very good agreement with numerical simulations. They show that the RO frequency does not explicitly depend on the details of the carrier-carrier scattering between QW and QD but strongly depends on the cavity lifetime $1/(2\kappa)$ and radiative recombination lifetime $1/W$. In contrast, the damping rate is crucially affected by the carrier-carrier scattering rates. For equal lifetimes of electrons and holes the damping increases with decreasing lifetimes. If both carrier types have different lifetimes τ_e and τ_h only the slowest species determines the damping rate while the effect of the fast species is negligible. For the case of fast holes and slow electrons that is important for comparison with experiments we found the following analytic relations using asymptotic techniques:
$\omega_{RO} = \sqrt{2N_{ph}W\kappa}$, $\quad \Gamma_{RO} \approx \frac{1}{2}\omega_{RO}{}^2\tau_h + \tau_e{}^{-1} + W(N_{ph} + N_h)$ where N_{ph} and N_h are the steady state values of the number of photons per QD and the occupation probability of the holes in the QD, respectively. This dependence of Γ_{RO} on τ_e and τ_h is in agreement with our investigations of QD lasers with doped carrier reservoir [P5], where we showed that increasing n-doping concentration leads to a decrease of the electron lifetime τ_e, which was at the same time accompanied by an increased damping. On the other hand, p-doping of the same device did not yield a higher RO damping, which is also explained by the analytics as decreasing the lifetime of the fast species (here the holes) does not significantly change the damping. As a consequence we are able to predict the performance of a QD laser, for instance, n-doping should be helpful to achieve high RO damping rates and thus flat modulation response curves.

(ii) Quantum dot semiconductor optical amplifiers (QD-SOAs)

The second part of the project B2 considered the modelling of quantum dot based optical amplifiers and was aimed at understanding their ultrafast gain recovery dynamics. Due to the very short time-scales (fs) found in the gain dynamics it was necessary to use a full nonlinear simulation of the coupled coherent polarization and population dynamics of carriers [P4]. Thus we used the semiconductor Bloch equations including microscopically calculated carrier-carrier scattering rates between the 2D carrier reservoir and the confined QD states. Our results were in good agreement with experiments on the gain recovery and the amplification of pulse trains performed in project C8 (Woggon). The ultrashort gain depletion was found to be sensitive against changes of the pulse area and the dephasing time of the microscopic polarization, while the injection current density mainly influences the non-coherent part of the gain recovery dynamics. A detailed analysis of the underlying carrier dynamics using phase space projections revealed desynchronized behavior of electrons and holes in the recovery dynamics of the QD SOA that is directly related to the different microscopic scattering rates [P4].

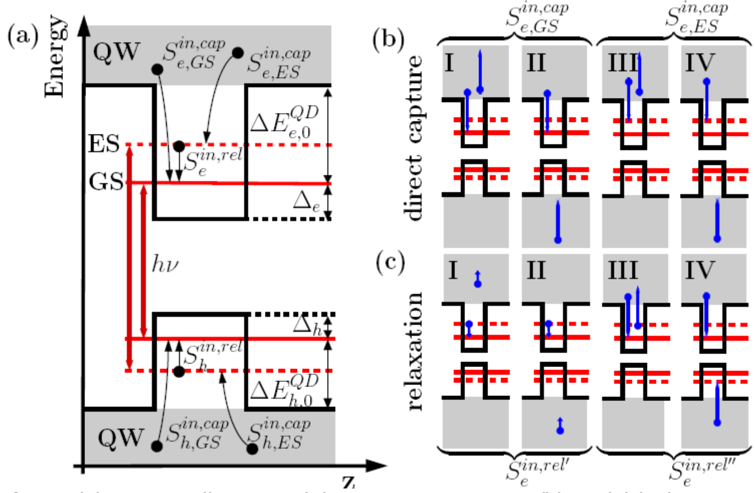

Fig. 5: (a) Energy diagram of the QD-QW system. (b) and (c) show direct electron capture and relaxation processes, respectively, from the QW to the GS (I,II) and the ES (III,IV). Panels I, III and panels II, IV show pure e-e and mixed e-h scattering processes, respectively. After [P3].

In a further step, we extended our model to include the first excited state (ES) of the QDs in addition to the QD ground state (GS) as shown in the band diagram in Fig.5a [P3]. By following the microscopic approach used before for the shallow QD (only one confined level in the QDs [P7]) we systematically included all possible Auger scattering processes between QW, ES and GS. We used microscopically based scattering rates obtained on the basis of a time-dependent perturbation approach [15]. The possible electron transitions that have been considered are shown in Fig. 5b for direct capture processes and in Fig.5c for relaxation processes with the blue arrows. The simulated gain recovery dynamics resulting from the extended model is plotted in Fig.6a for the three different Coulomb scattering channels sketched in Fig.6b. For case 1 we considered only direct capture processes, for case 2 direct capture into ES and relaxation into GS and for case 3 the complete set of all scattering processes. The in-scattering Coulomb rates that were implemented for relaxation processes between ES and GS, and for direct capture into the GS and ES are shown in Fig.6c and Fig.6d, respectively, as a function of the electron density w_e in the carrier reservoir. Note that all these Coulomb scattering processes involve two carriers (Auger processes). By analyzing the different scattering contributions that result from direct capture processes and from relaxation processes (see Fig.6a and b) we could show that the cascading process, where the carriers from the reservoir relax via the excited state makes a major contribution to the ultrafast recovery dynamics [P3]. Since this issue of direct capture and relaxation rates is controversially discussed in the literature, our microscopically based calculations could provide answers to those questions that might be of great general interest.

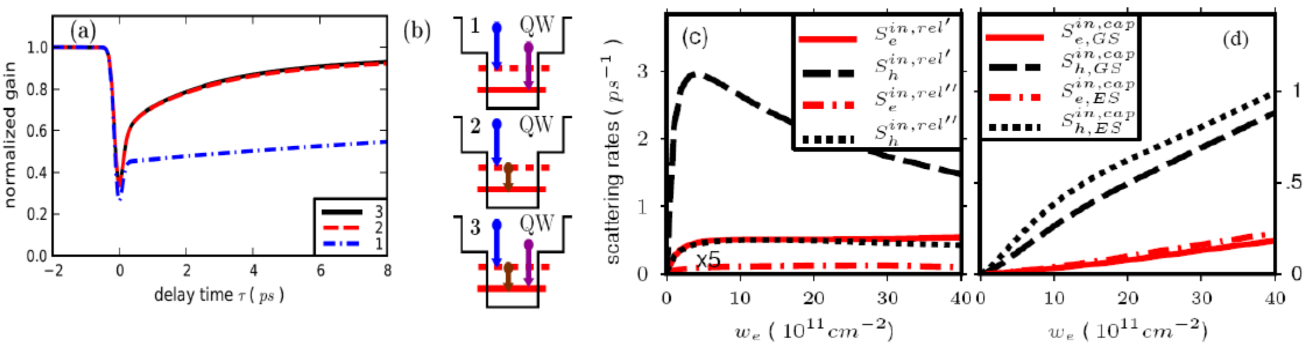

Fig. 6: (a) Ultrafast gain dynamics of QD optical amplifier for scattering scenario 1 (dash-dotted), 2 (dashed) and 3 (solid) as sketched in (b). Panels (c) and (d): Microscopically calculated Coulomb relaxation in-scattering processes between ES and GS $S_{e/h}^{in,rel}$, and in-scattering rates for capture into GS and ES $S_{e/h,GS/ES}^{in,cap}$, respectively, vs. QW carrier densities. After [P3].

References:

[1] H. Haug: *Optical Nonlinearities and Instabilities in Semiconductors*, Academic Press, (1988).

[2] C. H. Henry: *Theory of the linewidth of semiconductor lasers,* IEEE J. Quantum Electron. **18**, 259 (1982).

[3] J. Yang, P. Bhattacharya, and Z. Wu: *Monolithic integration of InGaAs-GaAs quantum-dot laser and quantum-well electroabsorption modulator on silicon*, IEEE Phot. Technol. Lett. **19**, 747 (2007).

[4] O. Qasaimeh, K. Kamath, P. Bhattacharya, and J. Phillips: *Linear and quadratic electro-optic coeffcients of self-organized $In_{0.4}$ $Ga_{0.6}$ As/GaAs quantum dots,* Appl. Phys. Lett. **72**, 1275 (1998).

[5] H. N. Klein, H. Chen, D. Hoffmann, S. Staroske, A. G. Steffan, and K. O. Velthaus: 1*.55 µm Mach-Zehnder modulators on InP for optical 40/80 Gbit/s transmission networks*, Conference Proceedings, 2006 International Conference on Indium Phosphide and Related Materials, **171** IEEE, Princeton, NJ, USA, (2006).

[6] V. Flunkert and E. Schöll: *Suppressing noise-induced intensity pulsations in semiconductor lasers by means of time-delayed feedback,* Phys. Rev. E **76**, 066202 (2007).

[7] M. Gioannini, A. Sevega, and I. Montrosset: *Simulations of differential gain and linewidth enhancement factor of quantum dot semiconductor lasers,* Opt. Quantum Electron. **38,** 381 (2006).

[8] W. W. Chow, and S. W. Koch: *Theory of semiconductor quantum-dot laser dynamics*, IEEE J. Quantum Electron. **41**, 495 (2005).

[9] V. Keldysh: *The Effect of a Strong Electric Field on the Optical Properties of Insulating Crystals,* J. Exp. Theo. Phys. **34**, 788 (1958).

[10] D. A. B. Miller, D. S. Chemla, T. C. Damen, A. C. Gossard, W. Wiegmann, T. H. Wood, and C. A. Burrus: *Band-edge electroabsorption in quantum well structures: The quantum-confined Stark effect*, Phys. Rev. Lett. **53**, 2173 (1984).

[11] J. D. Dow and D. Redfield: *Electroabsorption in semiconductors: The excitonic absorption edge*, Phys. Rev. B **1**, 3358 (1970).

[12] D. Merbach, E. Schöll, W. Ebeling, P. Michler, and J. Gutowski: *Electric field dependent absorption of ZnSe-based quantum wells: the transition from two-dimensional to three-dimensional behavior,* Phys. Rev. B **58**, 10709 (1998).

[13] K. E. Callan, L. Illing, Z. Gao, D. J. Gauthier, and E. Schöll: *Broadband chaos generated by an opto-electronic oscillator*, Phys. Rev. Lett. **104**, 11, 113901 (2010) (*highlighted in* Nature **465**, 41 (2010)).

[14] S. Melnik, G. Huyet, and A. V. Uskov: *The linewidth enhancement factor of quantum dot semiconductor lasers*, Opt. Express **14**, 2950 (2006).

[15] T. R. Nielsen, P. Gartner, and F. Jahnke: *Many-body theory of carrier capture and relaxation in semiconductor quantum-dot laser*s, Phys. Rev. B **69**, 235314 (2004).

[16] D. O'Brien, S. P. Hegarty, G. Huyet, and A. V. Uskov: *Sensitivity of quantum-dot semiconductor lasers to optical feedback,* Opt. Lett. **29**, 1072 (2004).

[17] V. Cesari, P. Borri, M. Rossetti, A. Fiore, and W. Langbein: *Refractive index dynamics and linewidth enhancement factor in p-doped InAs-GaAs quantum-dot amplifiers,* IEEE J. Quantum Electron. **45**, 579 (2009).

3.3.2 Project-related publications of the principal investigators

a) Peer reviewed publications in journals

[P1] B. Lingnau, K. Lüdge, E. Schöll, and W. W. Chow,
Many-body and nonequilibrium effects on relaxation oscillations in a quantum-dot microcavity laser,
Appl. Phys. Lett. **97,** 111102 (2010)

[P2] K. Lüdge, R. Aust, G. Fiol, M. Stubenrauch, D. Arsenijevic, D. Bimberg and E. Schöll,
Large Signal Response of Semiconductor Quantum-Dot Lasers,
IEEE J. Quantum Electron. **46**, 1755, (2010)

[P3] N. Majer, K. Lüdge, and E. Schöll,
Cascading enables ultrafast gain recovery dynamics of quantum dot semiconductor optical amplifiers,
Phys. Rev. B 82, 235301 (2010)

[P4] M. Wegert, N. Majer, K. Lüdge, S. Dommers-Völkel, J. Gomis-Bresco, A. Knorr, U. Woggon, and E. Schöll, *Nonlinear gain dynamics of quantum dot optical amplifiers*,
Semicond. Sci.Technol. **26**, 014008 (2011), invited paper.

[P5] K. Lüdge and E. Schöll,
Nonlinear dynamics of doped semiconductor quantum dot lasers,
Eur. Phys. J. D **58**, 167 (2010), invited paper.

[P6] C. Otto, K. Lüdge, and E. Schöll,
Modeling quantum dot lasers with optical feedback: sensitivity of bifurcation scenarios,
Phys. Stat. Sol. (b) **247**, 829 (2010), invited paper.

[P7] K. Lüdge and E. Schöll,
Quantum-dot lasers – desynchronized nonlinear dynamics of electrons and holes,
IEEE J. Quantum Electron. **45**, 1396 (2009), invited paper.

[P8] K. Lüdge, M. J. P. Bormann, E. Malic, P. Hövel, M. Kuntz, D. Bimberg, A. Knorr, and E. Schöll,
Turn-on dynamics and modulation response in semiconductor quantum dot lasers,
Phys. Rev. B **78**, 035316 (2008)

b) Other Publications

[P9] R. Kunert, E. Schöll, and U. W. Pohl,
Ordering Effects In Self-Organized Quantum-Dot Stacks,
Proceed. 30th Int. Conf. Phys. Semicond. (ICPS-30) Seoul 2010 (2010).

[P10] N. Majer, K. Lüdge, and E. Schöll,
Cascading enables ultrafast gain recovery dynamics of quantum dot semiconductor optical amplifiers,
Int. Nano-Optoelectronics Workshop (iNOW) Peking (2010)

[P11] K. Lüdge, E. Malic and E. Schöll, *The Role of Decoupled Electron and Hole Dynamics in the Turn-on Behavior of Semiconductor Quantum-Dot Lasers*
Proceed. 29th Int. Conf. Phys. Semicond.(ICPS-29), Rio de Janeiro 2008, AIP Conf. Proc. 1199, 475 (2009).

[P12] K. Lüdge, E. Malic, M. Kuntz, D. Bimberg, A. Knorr, E. Schöll,
Dynamic response of quantum dot lasers – Influence of nonlinear electron-electron scattering
IEEE Proc. of CLEO/QELSC, San Jose, USA, May 2008 Vol. 1-9 981 (2008)

3.4 Project outline

Objectives and methods

The aim of the project is to develop microscopically based models for QD laser and amplifier structures that are able to quantitatively describe complex integrated structures and at the same time allow for analytic insights into the underlying dynamic processes. This way we bridge the gap between highly sophisticated but computationally expensive QD modeling and phenomenological dynamical rate equation models that need a variety of fit parameters. We aim to further improve our existing microscopic model by taking into account the spectral properties of the inhomogeneously broadened gain medium due to the size distribution of the QDs as well as by including the effect of a dynamic amplitude-phase coupling (α-factor or linewidth enhancement factor [1,2]). Starting from the results of the last period concerning the quantitative modeling of solitary laser and amplifier devices as well as the results concerning the effect of a single feedback section we are going to investigate photonic integrated structures containing multiple feedback and modulator sections. With this we will describe and predict interesting and technologically useful dynamical phenomena. Self-organized quantum dot laser structures with integrated electro-optic modulators are attractive for applications in optical communication systems as well as in intra-chip and inter-chip optical interconnects [3] because electro-optic effects like the quantum confined Stark effect are particularly strong in QDs [4]. Integrated Mach-Zehnder (MZ) modulators are playing an important role for advanced modulation formats (e.g. Differential Quadrature Phase Shift Keying) which are promising for beyond 40 Gbit/s transmission [5], but have so far only been realized for conventional quantum well laser structures. Our aim is to extend such integrated structures to quantum dot systems. By using the predictive power of our model approach, we will break new ground.

A further aspect that will be studied in the project is the effect of noise on the dynamic behavior of the devices. The noise will be modeled on the basis of nonlinear stochastic differential equations of Langevin type describing the spontaneous emission in the device by a Langevin noise term. Here we can build on our previous expertise on noise-induced effects in conventional lasers [6]. The focus will be on the interaction of the noise with the time delays and the nonlinearities, as this could be a key element for designing and optimizing the device performance.

For the laser structures the electrical field will be modeled by nonlinear delay differential equations of Lang-Kobayashi type that are well suited for stability- and bifurcation analysis of the complex dynamic behavior. The dynamics of electrons and holes in the active region, i.e. inside the quantum dots, as well as the dynamics of the carriers in the surrounding reservoir will be modeled by microscopically based rate equations that consider the Coulomb interaction up to the 2nd order Born approximation. Extending our analysis to a systematic incorporation of Coulomb scattering involving also the excited state of the QDs, we will be able to investigate its effects on the dynamic behavior. In order to address spectral properties of the laser emission, the inhomogeneously broadened QD ensemble will be divided into several sub-ensembles modeled by separate rate equations for each group [7], which correspond to different laser energies. The results of the simulations will be compared to experiments obtained for VCSELs in project C1 (Hofmann, Bimberg) and for edge emitters in project C6 (Bimberg, Erbert).

Implementing optical injection into the extended model and investigating the resulting bifurcation diagrams will be one goal at the beginning of the project. We aim to understand how the underlying microscopic scattering processes determine the laser performance and how the results are different from those obtained with phenomenological rate equation models. At this point it is also planned to compare the results to those obtained by using dynamic many-body theory [P1] that is based upon the work of Chow et al.[8] for optically injected QD lasers. With this complementary approach the interplay between master-slave laser detuning, inhomogeneous broadening and renormalizing Coulomb effects will be investigated.

The next step of our project will be the modeling of multiple integrated feedback sections. One crucial issue for that is the correct implementation of the amplitude-phase coupling and the chirp in the device. We aim to derive these parameters from our work on dynamic many-body theory [P1] as well as from our amplifier simulations (see below), and implement them thereafter into the delay differential equations. As a result our microscopically based model will be able to predict the nonlinear dynamics and bifurcation scenarios of different integrated laser structures, and thus it will be possible to optimize the device performance. To achieve this predictive power, numerical tools for bifurcation analysis of the delay-differential equations (e.g. DDE-BIFTOOL) will be used. These path-following or continuation tools enable us to trace desired operating modes in the multi-dimensional parameter space. In parallel to the numerical simulation, asymptotic analytical methods, using time-scale separation of slow and fast dynamic variables, will be applied that allow us to derive analytical expressions for the occurring bifurcations and thus enable a better understanding of the underlying physical processes.

Besides integrated devices with multiple feedback sections we will incorporate integrated quantum dot based electro-optic modulators (EOMs). We aim to develop a microscopic model for these EOM devices within our project in close collaboration with the experimental projects C1 (Hofmann, Bimberg) and C6 (Bimberg, Erbert). EOMs are mostly either absorptive or refractive modulators. In absorptive electro-optic modulators the amplitude of the light beam is changed due to a manipulated absorption coefficient of the material, e.g. by the Franz-Keldysh effect [9], the quantum confined Stark effect (QCSE) [10], or excitonic absorption [11]. In refractive electro-optic modulators the phase of the light beam is shifted because of an electric field-induced change in the refractive index of the material, e.g. caused by the Pockels effect. A phase modulating EOM can also be used as an amplitude modulator through a Mach-Zehnder (MZ) interferometer [5], which consists of two parallel coherent light beams in one of which the phase is shifted electro-optically before both beams interfere. The modeling will benefit from our previous work concerning the QCSE in ZnSe-quantum wells [12] as well as the work concerning the chaotic dynamics in Mach-Zehnder-modulators with electro-optical feedback [13].

The second part of our project deals with QD based semiconductor optical amplifiers (SOAs). Because these devices do not consist of a resonator it is necessary to consider spatial propagation effects of the electric field inside the device. Moreover, our results of the last period underline that coherent effects of the microscopic polarization play a crucial role for the gain recovery dynamics. As a consequence the optical amplifiers will be modeled on the basis of the Maxwell-Bloch equations in traveling wave approximation which treats the fast microscopic electronic polarization of the QDs as a dynamic variable. This allows us to describe ultrafast dynamic effects like the gain recovery of the amplifier on a fs timescale as well as propagation effects of the electric field. By incorporating the microscopic Coulomb scattering rates between QD confined states and states in the surrounding carrier reservoir we will investigate pulse-shaping effects as a function of parameters like QD size, amplifier length and temperature as well as the chirp of the SOA if subjected to optical or electrical input pulses. The ultrafast gain dynamics and the optical switching as well as cross gain modulation and cross phase modulation will be optimized and compared to experimental results from projects C6 (Bimberg, Erbert) and A7 (Woggon). Using the results obtained in part (i) regarding the modeling of doped devices we will investigate the impact of doping on the gain dynamics and on the refractive index. Recent experiments [17] suggest that p-doping is efficient in reducing the α-factor but an adequate theoretical description is still missing. Another crucial point that will be stressed also in this part of the project is the investigation of the effect of noise, e.g., on the gain modulation (time jitter).

Additionally, we want to treat many-body effects within the screened Hartree-Fock approximation as presented in [8] and implement the resulting Coulomb renormalization into the simulation of quantum dot based semiconductor optical amplifier devices. This will allow us to calculate charge carrier interaction effects leading to a many-body renormalization of the energies of the corresponding charge carrier states within the semiconductor structure, changing the bandgap energy and influencing polarization and charge carrier dynamics. One advantage of this microscopic model is that it allows for the calculation of dynamical device parameters which are inaccessible in most rate equation models, such as the linewidth enhancement factor (α–factor) [2] and the chirp. These parameters strongly influence the behavior of QD-SOAs and the reaction of QD lasers to the injection of an external optical signal or to optical feedback [P6]. It has been proven difficult to reliably measure the α-factor experimentally especially in QD devices [14] because it is not a constant but sensitively depends on the operation condition of the laser. The model described above will be used to extract the α-factor as a function, for instance, of the pump current which will be very useful for the laser device simulations in the first part of the project. It is also planned to compare the theoretical results with experimental measurements of C6 (Bimberg, Erbert) and A7 (Woggon).

Methods:

- Calculation of microscopic carrier-carrier scattering rates within a Boltzmann equation approach
- Integration of coupled nonlinear delay-differential equations (nonlinear rate equations)
- Bifurcation analysis of the delay-differential equations with numerical continuation tools (e.g. DDE-BIFTOOL)
- Investigation of nonlinear stochastic differential equations of Langevin type to describe the spontaneous emission in the device.
- Asymptotic analytical methods for bifurcation analysis
- Modeling of the coherent dynamics in travelling wave approximation
- Analysis of dynamical instabilities, e.g., intensity pulsations induced by optical feedback

Work program and time schedule

The work program is split into two parts that will be investigated in parallel by two PhD students. The separation is according to the modeling of laser structures on the one hand, and optical amplifier structures on the other hand.

(i) Integrated multi-section quantum dot laser structures

Our starting point is the microscopically based five-variable model of an electrically pumped edge-emitting QD laser developed in the first period of this project:

$$\begin{aligned}
\dot{n}_e &= S_e^{in}(N^{QD}-n_e) - S_e^{out} n_e - WA(n_e+n_h-N^{QD})\,n_{ph} - \tfrac{W}{N^{QD}} n_e n_h \\
\dot{n}_h &= S_h^{in}(N^{QD}-n_h) - S_h^{out} n_h - WA(n_e+n_h-N^{QD})\,n_{ph} - \tfrac{W}{N^{QD}} n_e n_h \\
\dot{w}_e &= \tfrac{\eta}{e_0} j(t) - \tfrac{N^{sum}}{N^{QD}}\left[S_e^{in}(N^{QD}-n_e) - S_e^{out} n_e\right] - B\left(w_e\right) w_e w_h \\
\dot{w}_h &= \tfrac{\eta}{e_0} j(t) - \tfrac{N^{sum}}{N^{QD}}\left[S_h^{in}(N^{QD}-n_h) - S_h^{out} n_h\right] - B\left(w_e\right) w_e w_h \\
\dot{n}_{ph} &= -2\kappa n_{ph} + \Gamma WA(n_e+n_h-N^{QD})\,n_{ph} + \beta \tfrac{W}{N^{QD}} n_e n_h
\end{aligned}$$

where n_e and n_h are the electron and hole densities in the QDs, w_e and w_h are the electron and hole densities in the carrier reservoir (QW), and n_{ph} is the photon density, respectively. The density N^{sum} is twice the total QD density as given by experimental surface imaging (the factor of 2 accounts for spin degeneracy). N^{QD} denotes twice the QD density of the lasing QD group. As a result of the size distribution and fluctuations of the material composition of the QDs, only a subgroup matches the mode energies for lasing. It is noted that N^{QD} is not a constant but increases with increasing pump current due to the increasing number of longitudinal modes in the laser output [P2]. β is the spontaneous emission coefficient and Γ is the optical confinement factor. $B(w_e)$ is the band-band recombination coefficient that includes bimolecular spontaneous emission and Auger recombination inside the QW. W is the Einstein coefficient. The coefficient 2κ expresses the total cavity loss. j is the injection current density, e_0 is the elementary charge, and η is the current injection efficiency that accounts for the fact that one cannot inject any more carriers if the QW is already filled. The dynamics of the QD laser is strongly influenced by the nonlinear non-radiative carrier-carrier scattering rates S_e^{in} and S_h^{in} for electron and hole capture into the QD levels and S_e^{out} and S_h^{out} for carrier escape from the QD levels, respectively, that have been microscopically calculated within the project as a function of the dynamic QW electron and hole densities w_e and w_h [P7].

We will extend this model by including the first excited states of QD electrons and holes as dynamic variables as well as the inhomogeneous broadening via sub-ensembles of equally sized QDs. To this end we divide the total number of QDs into N groups with different optical transition energies, and describe each sub-ensemble by separate electron and hole densities labeled with a group index j and an index m for ground (GS) and excited state (ES). Thus we obtain a system of $4N + 3$ coupled nonlinear rate equations for the QD carrier densities and the QW carrier and photon densities. First, the turn-on dynamics and the small-signal and large signal modulation response of a solitary laser will be studied.

Next, optical injection will be implemented into the extended model, and the resulting bifurcation diagrams will be investigated. The main goal will be to understand how the underlying microscopic scattering processes determine the laser performance and how the results are different from those obtained with phenomenological rate equation models, where the scattering times are approximated by constant fit parameters. A variety of such models have been used in the literature, and it is important to determine their range of validity and compare them to our model which uses microscopically calculated carrier-carrier scattering rates which give strongly nonlinear scattering times depending upon the actual dynamical values of the QW carrier densities. For instance, in the simplest case of phenomenological modeling, only one sub-ensemble of QDs is considered, the excited state is neglected, and electron and hole densities are assumed to be equal (Cork-Brussels model [16]). By an asymptotic analysis it can be shown under which conditions our model reduces to this three-variable model.

We will also implement optical injection into a dynamic many-body theory of QD lasers at the level of the screened Hartree-Fock and relaxation-rate approximation, as used in Ref. [P1]. The investigation of the interplay between master-slave laser detuning, inhomogeneous broadening and renormalizing Coulomb effects will be the main goal. A comparison of this modeling approach with the Coulomb scattering model presented above will be drawn. Also, the effect of noise on the injection properties will be systematically studied.

In the second year we will establish a model for a QD based electro-optic modulator described by an absorptive coefficient that changes due to the quantum confined Stark effect. This effect is based upon the red shift of the optical wavelength and the decrease of the oscillator strength through the shift of the energy levels and the distortion of the wave functions in a quantum well when an electric field is applied. Furthermore, we will investigate a Mach-Zehnder (MZ) interferometer in a QD based structure and develop a dynamic model. The operation mode of the MZ modulator will be investigated in close collaboration with projects C1 (Hofmann, Bimberg) and C6 (Bimberg, Erbert) where experiments on electro-optic modulators embedded in QD structures are planned for vertical cavity surface emitting lasers (VCSELs) and edge emitters, respectively. We will compare electro-absorptive modulators and MZ modulators with respect to their dynamic properties. Numerical simulation as well as a bifurcation analyses will be performed. Also, noise will be added in the simulation in form of Gaussian white noise within a Langevin approach of spontaneous emission, and its impact on the power spectrum will be investigated.

In the third year we will study integrated structures with multiple optical feedback sections and electro-optic modulator sections. The interaction of several delayed feedbacks with different delay times promises quite complex dynamic behavior and chaotic scenarios. The bifurcations will be analyzed by direct integration of the nonlinear dynamic equations, as well as by numerical continuation techniques and linear stability analysis. Our results on QD lasers with a single optical feedback section have already established a sensitive dependence on the α-factor, as shown in Fig.4 above. Therefore, it is of interest to study the effect of a dynamic α-factor on the device performance for integrated structures with multiple time delays. Here an exchange with the results obtained for the dynamic α-factor in the second part of the project (see below) is planned.

Finally, we plan to explore the potential of integrated QD structures for pushing the speed limit beyond 40 Gbit/s transmission. Based on our modeling and simulation of various structures, the ultimate potential of optimization will be investigated in close collaboration with the experimental projects C1 (Hofmann, Bimberg) and C6 (Bimberg, Erbert). The role of crosstalk attenuation will have to be carefully evaluated.

Time schedule:

1st year: Laser dynamics with QD excited state and inhomogeneous broadening, optical injection, many-body effects

2nd year: QD based electro-optic modulators and Mach-Zehnder modulators, noise effects

3rd year: Integrated structures with multiple time delays, dynamic α-factor

4th year: Exploring the potential for beyond 40 Gbit/s transmission (crosstalk attenuation)

(ii) Quantum dot based optical amplifier structures

In a semiconductor optical amplifier (SOA) the facet reflectivity is so low that the electrically pumped device is operated below the laser threshold. Optically injected pulses are amplified by the active gain material.
We will investigate the gain recovery dynamics in response to ultrashort optical input pulses in close collaboration with pump-probe experiments performed in projects A7 (Woggon) and C6 (Bimberg, Erbert). The theoretical model is based upon the Bloch equation approach for the coupled polarization and population dynamics of the QDs, since the ultrashort timescales require a coherent description based upon the density matrix. The dynamic equations for the QD interband polarization p_m^j, the QD electron and hole occupation probabilities $f_{e,m}^j$, $f_{h,m}^j$, and the QW electron and hole densities w_e, w_h, respectively, and the traveling wave field equation are given below. The QD ground state and excited state are labeled by m while j numbers the sub-ensemble of the inhomogeneously broadened QD distribution that has a QD density of $N^{QD,j}$. The microscopic polarization p_m^j is a dimensionless quantity describing the probability of a coherent optical transition between the respective electron and hole levels. T_2 is the dephasing time of the optical polarization, which accounts for coherence loss through scattering processes. The total macroscopic polarization density P is obtained by summing over all states and sub-ensembles (see equation on the right), where d is the thickness of the active region. The detuning of the input light field frequency towards the frequency of the optical transition of the respective QD level is given by $\delta\omega_m^j$. The Rabi frequency of the QD transitions with associated dipole moment µ (assumed to be equal for all QDs and all optical transitions) is given by $\Omega(t) = \frac{\mu}{\hbar} E(t)$, where $E(t)$ is the electric field envelope. R_{sp} is the spontaneous recombination rate assumed to be bimolecular as used in part (i) of this project. An important contribution to the dynamics of QD SOAs is the non-radiative carrier-carrier scattering rate between confined QD states and continuous 2D QW states denoted by $\left.\frac{\partial f_{e,m}^j}{\partial t}\right|_{col}$, that contains all Auger scattering processes between the confined QD levels and the carrier reservoir. The electric current density $j(t)$ is injected into the QW. In the field equation v_g is the group velocity of light, Γ is the optical confinement factor, and μ_0, ω_0, c_n are the absolute permeability, the optical center frequency, and the phase velocity of light, respectively.

Dynamic equations:

$$\frac{\partial p_m^j}{\partial t} = -i\delta\omega_m^j p_m^j - i\frac{\Omega}{2}\left[f_{e,m}^j + f_{h,m}^j - 1\right] - \frac{1}{T_2} p_m^j$$

$$\frac{\partial f_{e,m}^j}{\partial t} = -\mathrm{Im}\left[\Omega\, p_m^{j*}\right] - R_{sp} + \left.\frac{\partial f_{e,m}^j}{\partial t}\right|_{col}$$

$$\frac{\partial f_{h,m}^j}{\partial t} = -\mathrm{Im}\left[\Omega\, p_m^{j*}\right] - R_{sp} + \left.\frac{\partial f_{h,m}^j}{\partial t}\right|_{col}$$

$$\frac{\partial w_e}{\partial t} = \frac{j(t)}{e_0} - \tilde{R}_{sp} - 2\sum_{m,j} N^{QD,j} \left.\frac{\partial f_{e,m}^j}{\partial t}\right|_{col}$$

$$\frac{\partial w_h}{\partial t} = \frac{j(t)}{e_0} - \tilde{R}_{sp} - 2\sum_{m,j} N^{QD,j} \left.\frac{\partial f_{h,m}^j}{\partial t}\right|_{col}$$

Traveling wave field equation:

$$\left(\frac{\partial}{\partial z} + \frac{1}{v_g}\frac{\partial}{\partial t}\right) E(z,t) = \frac{1}{2}\Gamma i \mu_0 \omega_0 c_n P(z,t)$$

with $$P(z,t) = 2\sum_{j,m} \frac{N^{QD,j}}{d} \mu p_m^j$$

First, we will investigate the spatiotemporal dynamics of pulse propagation in an optical amplifier for different device parameters such as amplifier length, QD size, QD density, operation temperature and injection current for different optical input signals with varying pulse shape, pulse width, input power and pulse repetition rate. The goal is to influence the pulse shaping characteristics of the device and tailor temporally and spectrally narrow output signals without significant patterning effects.

In a next step we will implement many-body effects at the level of screened Hartree-Fock approximation in collaboration with our external partner Weng Chow [P1] into the simulation. The many-body effects lead to renormalizations of the single-particle energies of QD and WL states causing a shift of the optical transition frequency as well as shifts in the intrinsic Rabi frequency.

Furthermore, we will extract the dynamic chirp and the dynamic α-factor from the coupled dynamics of electric field E and polarization P given by the above equations. The α-factor describes the amplitude-phase coupling of the optical field and is given as:

$\alpha(\omega) = -\dfrac{d\,\mathrm{Re}[\chi(\omega)]/dn}{d\,\mathrm{Im}[\chi(\omega)]/dn}$, where $\chi(\omega) = P(\omega)/(\varepsilon_0 E(\omega))$ is the electric susceptibility of the medium and n is the carrier density. In the spirit of hierarchical modeling, we will provide look-up tables of the dynamic α-factor as a function of the dynamic variables. These can be implemented, for instance, into the delay-differential equations describing the integrated multi-section laser structures studied in part (i) of this project (see above).

In the second year we plan to simulate the optical switching dynamics of the amplifier. We will simulate optical eye pattern diagrams, which give the large-signal optical response of the amplifier to random sequences of optical input bit patterns. In these diagrams the response to the random bit pattern is superimposed such that "open eyes" correspond to good amplification features. Furthermore the cross-phase and cross-gain modulation will be analyzed in dependence upon the inhomogeneous broadening of the gain medium.

In the third year we will investigate various integrated structures of QD based semiconductor optical amplifiers. We will combine our models to describe coupled amplifier and modulator sections, passive feedback and absorber sections in photonic integrated circuits. Time delay effects due to light propagation between different parts of the structure play an important role, and can lead to highly complex nonlinear dynamics. The dynamic response and the occurring instabilities and bifurcation scenarios will be systematically studied, in order to predict optimal properties of a structure. Furthermore the effect of using a doped carrier reservoir upon the amplifier performance will also be studied in detail. Thus we will model gain and index changes that result from a built-in carrier reservoir and explore its potential to reduce the α-factor or to achieve ultrafast cross-phase modulation without patterning effects.

Finally, the effect of noise upon the features of the SOA will be systematically studied. To include the noise the field equation has to be transformed into a stochastic differential equation of Langevin type. This is done by adding a Gaussian white noise source that is scaled with the spontaneous emission rate, i.e. $F^E(t)$, to the right hand side of the traveling wave equation given above. Here $F^E(t) = F_1^E(t) + iF_2^E(t)$ is a complex valued fast fluctuating random number with zero mean. It is statistically independent for different times t and t', and has statistically independent real and imaginary part. These properties are described by:

$$\langle F^E(t)\rangle = 0\ , \quad \langle F_l^E(t), F_m^E(t')\rangle = \frac{1}{2}\beta R_{sp}\delta_{lm}\delta(t-t') \quad \forall t,t' \in R, \quad l,m \in \{1,2\}$$

Spontaneous emission or fiber-to-fiber noise are prominent sources of noise. In particular, it is of interest to discuss the bit error rate, which is an important characterization of the quality of the SOA with respect to applications in optical communication technology. Ways of reducing the destructive influence of noise by appropriate tailoring of the QD structure have to be explored. It is well known that the interplay of noise, delay, and nonlinear dynamics can often produce unexpected effects like suppression of noise or control of noise-induced oscillations, or even stochastic resonance or coherence resonance. Optimizing the integrated structure will be a significant task.

Time schedule:

1st year: Pulse shaping and pulse propagation in an optical amplifier,
dynamic chirp and α-factor, many-body effects

2nd year: Optical switching dynamics, cross-phase and cross-gain modulation

3rd year: Integrated amplifier structures. Devices with doped carrier reservoir.

4th year: Noise effects (gain modulation, bit error rate)